Multi-Step Forward Dynamic Gait Simulation

Matthew Millard, John McPhee, and Eric Kubica

Systems Design Engineering, University of Waterloo, 200 University Ave West, Waterloo ON, Canada
E-mail: mjhmilla@engmail.uwaterloo.ca

Summary. A predictive forward-dynamic simulation of human gait would be extremely useful to many different researchers, and professionals. Metabolic efficiency is one of the defining characteristics of human gait. Forward-dynamic simulations of human gait can be used to calculate the muscle load profiles for a given walking pattern, which in turn can be used to estimate metabolic energy consumption. One approach to predict human gait is to search for, and converge on metabolically efficient gaits. This approach demands a high-fidelity model; errors in the kinetic response of the model will affect the predicted muscle loads and thus the calculated metabolic cost. If the kinetic response of the model is not realistic, the simulated gait will not be reflective of how a human would walk. The foot forms an important kinetic and kinematic boundary condition between the model and the ground: joint torque profiles, muscle loads, and thus metabolic cost will be adversely affected by a poorly performing foot contact model. A recent approach to predict human gait is reviewed, and new foot contact modelling results are presented.

1 Introduction

Human and animal gait has been studied by using experiments to tease out the neural, muscular and mechanical mechanisms that are employed to walk. Inverse dynamic simulation is the most common simulation technique used to study human gait. Inverse dynamics works backwards from an observed motion in an effort to find the forces that caused the motion – inverse dynamics is not predictive. In contrast, forward dynamics can be used to determine how a mechanism will move when it is subjected to forces – making forward dynamics predictive.

Forward dynamic human gait simulations usually only simulate a single step [4,11] in an effort to avoid modelling foot contact and balance control systems. The few multi-step forward-dynamic simulations in the literature have used a relatively fixed gait [24, 27]. In contrast, Peasgood et al.'s [23] forward dynamic simulation is predictive: the simulated gait is altered in an effort to

C.L. Bottasso (ed.), *Multibody Dynamics: Computational Methods and Applications,* 25

find metabolically efficient or 'human-like' gaits, allowing it to estimate how a person would walk in a new situation – e.g. with a new lower-limb prosthetic, or more flexible muscles.

A computer simulation that is able to reliably predict how a person would walk in a new situation would be extremely useful to many health care professionals and researchers studying human gait. Peasgood et al.'s system finds 'human-like' or metabolically minimal gaits by searching for joint trajectories for the hip, knee and ankle that minimize metabolic cost per distance traveled. The model is not supported or balanced by any artificial means, and so, poorly chosen trajectories can overwhelm the balance controller, causing the model to fall. This study was undertaken to evaluate and extend Peasgood et al.'s work, and to identify the shortcomings of current multi-step forward dynamic gait simulations.

2 Methods

Peasgood et al.'s system represents the first attempt at developing a predictive, multi-step gait simulation that searches for metabolically efficient gaits. Nearly 1,000, ten-step simulations were required to find a metabolically efficient, 'human-like' gait. Originally the 1,000 gait simulations took 10 days to perform on a single computer using the popular mechanical modeling package MSC.Adams [21]. DynaFlexPro [9], another modeling package, developed since Peasgood et al.'s work, offers substantial performance advantages over Adams: the updated version of Peasgood et al.'s predictive system now takes only 8 hours to run. Peasgood et al.'s work was taken, carefully examined, analyzed, improved and implemented in DynaFlexPro.

2.1 Dynamic Model

Peasgood et al. developed a predictive gait simulation using a 2D, seven segment, nine degree of freedom (dof), anthropomorphic model shown in Fig. 1 with a continuous foot contact model. This is a fairly standard model topology for gait studies. The upper body is simplified into a single body representing the head, arms and trunk (HAT); the thigh and shank are each one segment, as is the foot [1, 3, 13]. An additional simplification has been made in this model by fusing the HAT to the pelvis. There was an unintended error in Peasgood et al.'s original model: there was an extra body attached to the foot that had a moment of inertia of 1.5 kg m^2, which is comparable to the HAT segment.

A convergence study was performed on both the DynaFlexPro and the corrected Adams gait models by dropping both unactuated models onto the floor from the same initial conditions. The convergence of each model was checked individually. The results from the DynaFlexPro model converged for every simulation, whereas the Adams model failed to converge with an integrator

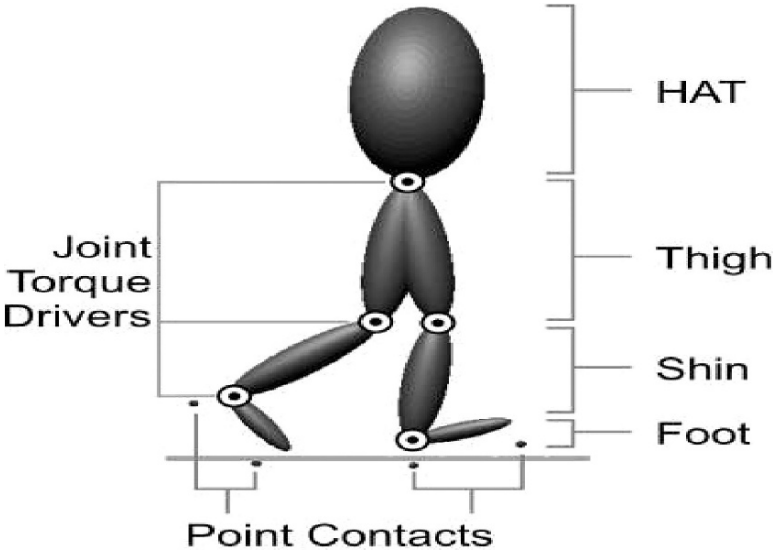

Fig. 1. Peasgood et al.'s seven segment, nine degree of freedom, planar gait model with a 2-point continuous foot contact model

Table 1. Performance comparison between the Adams and DynaFlexPro 2D seven segment gait models for a 10 second simulation. The Adams simulation with an integrator error tolerance of 10^{-5} failed to converge. The relative error increases from the hip position to the foot angle: the large mass of the HAT attenuates position error of the hip, while foot position is more sensitive to errors due to its light mass. The stiffness of the heel contact makes the simulated contact forces very sensitive to errors

	Adams	DynaFlexPro	Maximum relative error (%)		
Integrator	GSTIFF (I3)	ode15s (NDF)	Left hip	Right ankle	Right heel
error tol.	Simulation time		disp. (x)	angle	contact force
10^{-5}	29	4.1	3.02	5.65	14.30
10^{-7}	33	7.3	0.09	0.16	0.27
10^{-9}	36	30	0.24	0.48	0.73

error tolerance of 10^{-5}. The maximum relative error between the Adams and DynaFlexPro result sets is shown in Table 1 for the horizontal position of the left hip, the angle of the right ankle and the contact force developed under the right heel. The relative error was computed by taking the largest absolute difference between the two simulations and dividing it by the largest absolute value from the DynaFlexPro result set. Interestingly, the simulations with an integrator error tolerance of 10^{-7} had the smallest relative error, and allowed the DynaFlexPro model to simulate four times faster than the Adams model as shown in Table 1.

2.2 Foot Contact

Foot contact forces were calculated using a two-point foot contact model, with a point contact located at the heel and metatarsal. Normal forces were calculated using the Adams implementation [22] of the continuous Hunt-Crossley [18] point contact model:

$$f_n = -ky^p - c(y)\dot{x}. \tag{1}$$

The Hunt-Crossley contact model calculates normal force (f_n) as a function of penetration depth (y), penetration rate ($\dot{y}$), material stiffness (k, p), and material damping ($c(y)$). The implementation of the model ramps up damping ($c(y)$) as a function of penetration depth, to prevent an instantaneous normal force that would be created using a simple damping term such as ($c_{max}\dot{y}$). A dry Coulomb model was used to calculate the force of friction between the points and the plane:

$$f_f = \mu(\dot{x})f_n. \tag{2}$$

This friction model has stiction (μ_s) and dynamic friction (μ_d) values that are interpolated using a cubic step function [22] between the stiction velocity (v_s) and the sliding velocity (v_d) using the tangential contact velocity ($\dot{x}$) as an input. The particular contact and friction parameters used for the gait simulation were chosen by the pattern search routine (described later) to match the ground reaction forces created during healthy gait [26].

2.3 Joint Trajectory Control

Pre-computed joint trajectories are used to define the gait of the model at the position level. Each joint is actuated using a proportional-derivative (PD) controller that modifies and regulates the predefined joint trajectories. The initial joint trajectories were taken from an existing experimental data set of a healthy gait of an average-sized male [26] and interpolated using a five-term Fourier series:

$$\theta_j(t) = C_0 + \sum_{k=1}^{5}\left[A_k sin\left(\frac{2\pi kt}{period}\right) + B_k cos\left(\frac{2\pi kt}{period}\right)\right]. \tag{3}$$

Some adjustments were made to the trajectories in order to apply them to a sagittal plane gait model: the swing phase of the ankle trajectory had to be altered to prevent the foot from dragging on the ground. This makes sense because the 2D sagittal plane model cannot use hip roll and body sway in the frontal plane to adjust the floor clearance of the swing limb, unlike the subject used in the experiment data set. The interpolated joint trajectories were applied to the PD joint controllers to achieve an initial simulated gait. The optimization routine adjusts the values of the Fourier series coefficients for each limb to search for new gaits. The same Fourier coefficients are used for each limb, offset in phase by π radians, restricting the model to walk with a symmetric gait.

2.4 Balance and Velocity Control

A balanced gait and a desired forward velocity is achieved by manipulating the pitch of the HAT. The pitch controller works by monitoring the orientation of the HAT relative to a desired set angle and speeding up or slowing down the progression of the legs through the joint trajectories to keep the HAT at a desired angle. When the HAT pitches forward (backward) beyond the desired set angle, the legs are driven faster (slower) to walk ahead (behind) of the HAT. The velocity controller is very similar to the pitch controller: when the model is moving too slowly (quickly), the reference angle for the pitch controller is increased (decreased), causing the model to lean forward (backward), making the balance controller force the model to walk faster (slower). A detailed account of the pitch and velocity controllers can be found in Peasgood et al.'s original paper [23]. The pitch and velocity controllers balanced the model, but only over a very narrow range: the model could not initiate gait from a stand still, but had to begin the simulation with carefully selected initial conditions. These initial conditions were used for every simulation.

2.5 Pattern Search Optimization Routine

Peasgood et al. tuned the control system parameters and the joint trajectories using a pattern search optimization routine. The algorithm is conceptually described below. A more formal treatment of the material can be found in Lewis et al. [20].

1. Repeat for all parameters:
   (a) Add amounts $+\Delta$ and $-\Delta$ (called the grid size) to one parameter.
   (b) Evaluate the objective function. Save parameter changes that improve the objective function for later use.
2. Update all parameters with the improved values from Step 1.
3. Evaluate the objective function. If it improves, accept the new parameter set from Step 2; else use the original parameter set.
4. Decrease Δ by half, return to Step 1. Continue until Δ is below a predefined tolerance.

The performance of this algorithm relies on the assumption that a set of individual changes to the joint trajectories will collectively result in an improvement. This assumption is valid if the set of parameters are independent. Peasgood et al.'s assumption of independence does not hold when applied to joint trajectories: a beneficial change to the hip joint trajectory may cause the model to fall when combined with a beneficial change to the knee joint trajectory. Thus this search routine only ever improved the objective function when a set of individual parameter changes was found that just happened to collectively improve the simulated gait.

The pattern search optimization routine was used to find joint trajectories that minimized metabolic cost. In an optimization run that had 717 simulations only once did all of the individual improvements found by the pattern search routine result in a more efficient gait when used collectively. This one single improvement was able to decrease the metabolic cost of the simulated gait by 21.5%. An examination of the optimization log file revealed that there were many individual parameter changes that improved the objective function but were ignored. Further investigation showed that a set of individually beneficial parameter changes caused the model to fall when applied simultaneously. The pattern search algorithm was adjusted to take advantage of good individual parameter changes immediately, resulting in a greedy pattern search routine. A further adjustment was made by allowing the pattern search to continue making adjustments to a single parameter that improved the objective function until the improvements ceased.

3 Results

The joint angles for the final simulated gait and a healthy human gait [26] are shown in Fig. 2. The standard deviation of the joint angles, torques and ground reaction forces for the current results are negligible, indicating that the gait is very consistent. The joint trajectories of the knee and hip are similar between all three data sets, but the ankle joint trajectories, and torques are quite dissimilar. The log file of the optimization routine revealed that increasing the ankle extension led to a significant reduction in metabolic cost. The adjusted pattern search routine was able to find a gait that resulted in 47.6% less metabolic cost, a 26.1% improvement over Peasgood et al.'s original approach.

The foot contact model produced ground reaction forces that differ substantially from those observed during normal human gait [26], as shown in Fig. 3. The poor performance of the foot contact model is partly responsible for the joint torque differences seen between healthy human gait and the simulated results in Fig. 2. The kinematics of the foot contact model also exhibited heel and metatarsal compressions exceeding 40.0 mm, far greater than compression levels of real human heel [10] and metatarsal pads [7]. The kinematics and kinetics of this gait differ from healthy human gait [26], and are highly influenced by differences between the simulated foot contact model and a human foot.

4 Discussion

One of the biggest shortcomings of the current system is that the balance controller is so sensitive to changes in gait parameters, that very little of the gait space can be searched without making the model fall. The latest optimization run consisted of 721 simulations; 543 of these simulations resulted in the

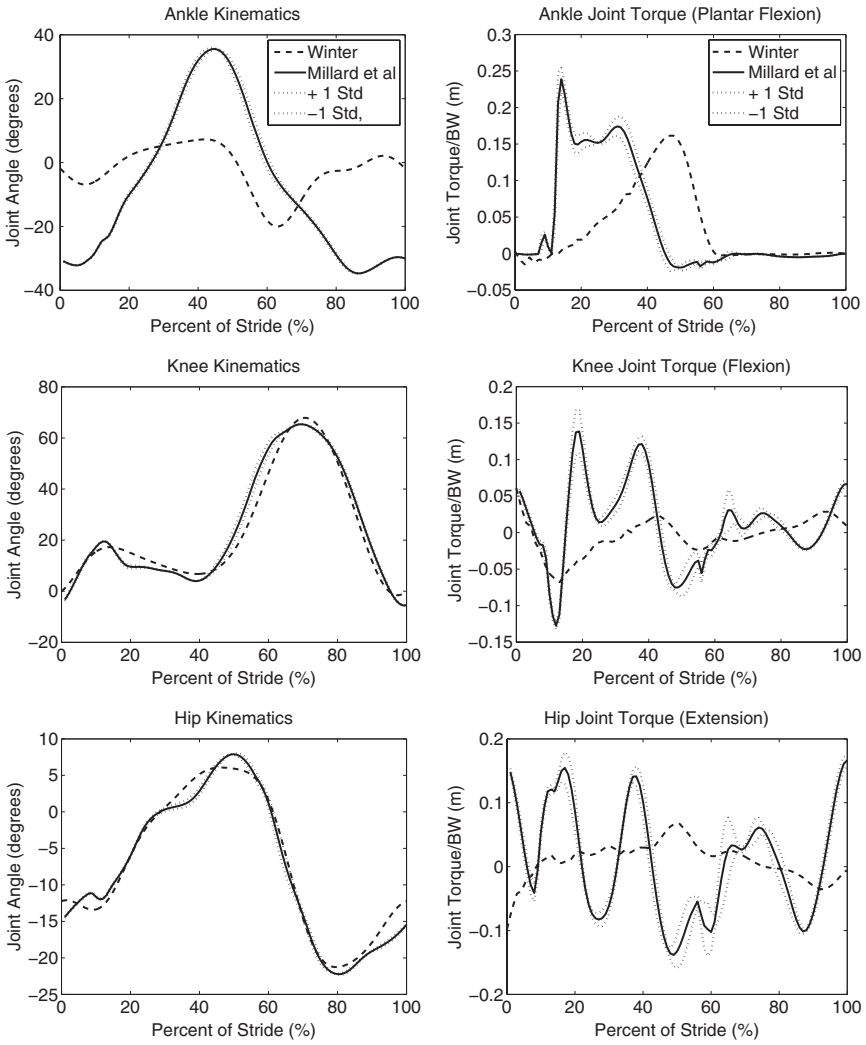

Fig. 2. Joint trajectory and torque comparison between Winter's recordings of human gait [26], and the current results

model falling. As well, the current system is not well suited to making changes to single parameters without having potentially disastrous effects: changing any one of the Fourier coefficients will alter the entire gait cycle. A parameter change that improves the efficiency of the stance phase, may cause the model to fall during the swing phase. A more advanced balance control system that allows the swing and stance phases to be tuned separately would be a great improvement to the current system.

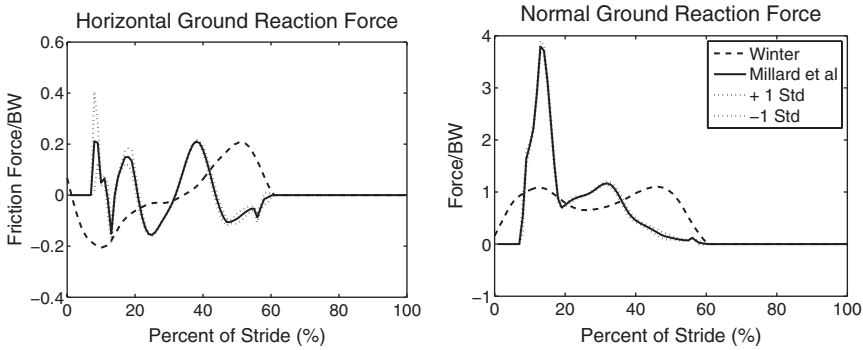

Fig. 3. Normal and friction force comparison between Winter's recordings [26] and the current two-point foot contact model

The computationally efficient, but low-fidelity foot contact model produced ground reaction forces and foot pad compressions that were drastically different than those observed in healthy human gait, and negatively affected the simulated joint kinetics. A high-fidelity foot contact model is especially important for a predictive gait simulation: contact forces at the foot will affect the loads at the joints of the legs, and thus the metabolic cost of the leg muscles. If the model does not have a realistic foot contact model, it will be impossible to produce metabolic cost estimates that correspond to what one would expect from a human [28]. A predictive gait simulation without a high-fidelity foot contact model could not converge to a 'human-like' gait.

5 Foot Contact Modeling

Foot contact models are typically not validated separately from the gait simulation [23, 24, 27]. This approach is problematic: if the ground reaction force representation is poor, it is impossible to know if its due to an error in the foot contact model or due to the way the foot is being used by the assumed control system. The only foot contact model that was validated separately from the gait simulation [12] was validated in a naive way: ankle joint torques and forces estimated from an inverse dynamics analysis were applied to a forward dynamic simulation of the foot model; the fidelity of the foot model was evaluated by comparing the kinematics of the simulated foot to the experimental data. This approach is naive because the quantization and measurement error that is inherent in an experimental inverse dynamics analysis will cause the forward dynamic simulation to diverge from the experimental observations, even if the model is perfect. None of the lumped-parameter foot contact models published to date [12, 23, 24, 27], provide convincing results of emulating a real human foot.

The approach taken in the current work to assess candidate foot contact models is different from previous attempts [12]: a contact model that was suitable for modeling heel tissue was first identified, then candidate foot contact models were created using this contact model. Ground reaction force profiles were used assess the fidelity each model: a realistic foot contact model should develop the same ground reaction forces as a human foot when driven through the same kinematic path. A simple experiment was undertaken to gather the data required to test the candidate foot contact models: a subject's ankle position and ground reaction force profiles during normal gait were recorded using Optotrak infrared diodes (IREDs) and a force plate. The subject walked at three different subjective paces (slow, normal and quickly) in two different load conditions: bodyweight (BW) and 113% bodyweight. The different velocity and loading conditions were used to assess the sensitivity of the model to cadence and load. The heavier loading condition was achieved by having the subject carry a cinder block. The following sections will detail recent work to create and validate a new foot contact model.

5.1 Foot Pad Contact Properties

Studies to determine the stiffness and damping properties of human foot pads have failed to produce consistent results. Traditionally *in vivo* experimental results disagree by orders of magnitude from *in vitro* experiments. In the past, *in vivo* experiments have measured the tissue compression and load by impacting an instrumented mass into a subject's heel [19, 25]. As long as the skeletal system of the body acts like a perfect ground, the deceleration of the mass will be entirely due to the compression of the heel pad. Aerts et al. [2] was able to experimentally demonstrate that this assumption is invalid: significant amounts of energy is lost through the body, skewing the stiffness values reported from *in vivo* pendular experiments to be nearly one-sixth the published *in vitro* values. *In vitro* stiffness and damping estimates obtained using an Instron material testing machine are also suspect because the tissue may not be representative of living foot pad tissue from the general population. An *in vivo* experimental procedure was developed to estimate foot stiffness and damping:

1. The compression of the heel pad was inferred by tracking the position of the fibular trochlea of the calcaneus using an Optotrak IRED. The fibular trochlea of the calcaneus is a bony protrusion on the lateral side (outside) of the heel bone. A marker was also placed on the medial (inside) side of the calcaneus.
2. The force acting on the heel pad was measured using a force plate. Only the heel was placed on the force plate.
3. The subject voluntarily lowered their heel on the force plate at three subjective speeds: slow, medium and fast. The heel was slowly raised. The fast trials had to be discarded due to undersampling, despite sampling the data at 200 Hz.

This experimental method assumes that there is not significant IRED marker movement relative to the calcaneus. The distance between the lateral and medial calcaneus markers was examined to estimate skin stretch: the distance of 68.0 mm changed by 2.0 mm on average during a load cycle, indicating that skin stretch has likely skewed the data. The hysteresis loops obtained during the preliminary experiment have energy losses ranging from 21–37%. This level of energy dissipation is somewhat similar to the 17–19% reported by Gefen et al.'s *in vivo* study [10] and grossly lower than the 46.5–65.5% reported by Aerts et al. Direct measurement of the heel pad tissue compression will be needed in order to produce more precise results.

5.2 Volumetric Contact Model

Theoretical contact modelling is a very active research area [16], with relatively sparse experimental work [8,14]. Unstable normal directions is one of the numerical problems that can arise during the simulation of contacting bodies with complicated geometry. A new contact model based on *interpenetration volumes* [16] has been developed to overcome many of the numerical instabilities of existing contact models and is currently being used by the Canadian Space Agency to simulate Canadarm operations. This contact model was chosen as an ideal candidate for a new foot contact model because of its desirable numerical properties.

Gonthier et al. [16] analytically derived expressions for the normal force $\boldsymbol{f}_n$, and rolling resistance $\boldsymbol{\tau}_t$ for a linearly elastic Winkler foundation of stiffness k and damping a impacted by a body with a normal velocity of v_{cn}:

$$\boldsymbol{f}_n = kV(1 + av_{cn})\hat{\boldsymbol{n}}, \tag{4a}$$

$$\boldsymbol{\tau}_t = ka\boldsymbol{J}_c \cdot \boldsymbol{\omega}_t. \tag{4b}$$

These very general expressions assume it is possible to calculate the volume of interpenetration (V), and its inertia matrix ($\boldsymbol{J}_c$). These parameters can be very challenging to compute for arbitrarily shaped bodies, and so analytical expressions for V and $\boldsymbol{J}_c$ were developed for spherical primitives. The foot contact model was then created out of an array of spherical elements. Vectors and matrices are shown in boldface; scalars in regular type.

Although it is often reported that human heel tissue stiffness is dependent on strain [17] (using a penetration depth model), it is not clear if this dependence is due to geometry of the pad or the tissue itself: V is a nonlinear function of penetration depth, and might account for the nonlinearity of the heel response. A preliminary study using the experimental procedure described in the previous section was undertaken to garner *in vivo* hysteretic load curves of the heel. A single spherical element was chosen to represent the heel pad. The stiffness and damping parameters were tuned to try to make the response of the model match the experimental data set. Due to the nonlinearity of the problem, a full-enumeration optimization routine was used to

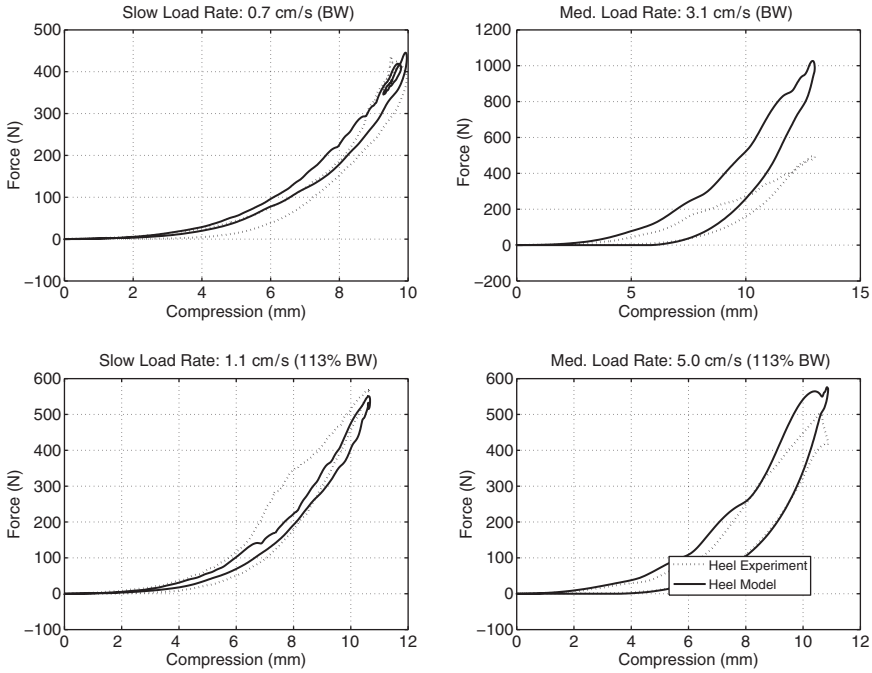

Fig. 4. Compression load cycles of a tuned volumetric sphere vs experimental data. Stiffness and damping are constant. The label 'BW' stands for body weight, and the load rate reported is the maximum normal velocity the heel achieves as it contacts the floor

find a good set of parameters for the simulated heel pad. The results shown in Fig. 4 show that a single volumetric spherical contact element was able to achieve a good agreement with the experimental *in vivo* load curves in all but one of the trials. Since there were so few experimental trials undertaken it is impossible to know if the ill-fitting trials is a consequence of the 'memory' of foot tissue observed *in vitro* [2], or due to a fundamental difference between the contact model and the contact properties of human heel pads. The preliminary results were encouraging enough to pursue a foot contact model using Gonthier et al.'s linearly elastic volumetric contact model and spherical contact elements.

5.3 Friction Modeling

Every foot contact model developed to date has made use of a Coulomb friction model without any experimental justification. There has not been any effort to date to develop experiments to determine the shear and friction properties of human heel pad *in vivo* or *in vitro*. Typically the tangential ground reaction forces found in simulated feet are accompanied by unrealistically high initial transient forces [12,24], or in the very least force profiles that

deviate [23] from experimental ground reaction force recordings [26]. Initially a Coulomb model was adopted to see how it would perform with the new foot contact models.

5.4 Foot Contact Modelling Results

Contact force computation and simulation usually represents a large computational burden when simulating a dynamic system. Thus a simple, yet high-fidelity foot contact model is very desirable. Accordingly foot contact model topologies began from the very simple and progressed in complexity as shown in Fig. 5 to achieve the desired fidelity.

Two-dimensional foot contact models were driven at the ankle through experimentally gathered foot trajectories. An optimization routine was used to tune the contact and friction properties of every spherical element, and to make slight adjustments to the geometry of the foot. It is important to note that the slight flex through the mid foot at the tarsal joints [5] is not being modelled: simulating this flexure could be computationally expensive due to the stiff nature of the foot.

5.5 Two-Sphere Single Segment Foot Contact Model

The first contact model tested consisted of a single-segment rigid foot with a volumetric spherical contact for the heel and the metatarsal shown in Fig. 5a, with a Coulomb friction model. The foot was tuned to fit all of the trials normal and friction force profiles. The normal ground reaction forces of best fit are shown in Fig. 6. Curiously the model was able to fit the faster paced trials far better than the slow trials, which show some significant deviations. The optimization routine found a solution that yielded metatarsal penetration depths that were nearly 20.0 mm – far greater than the 7.0 mm observed in other studies [7].

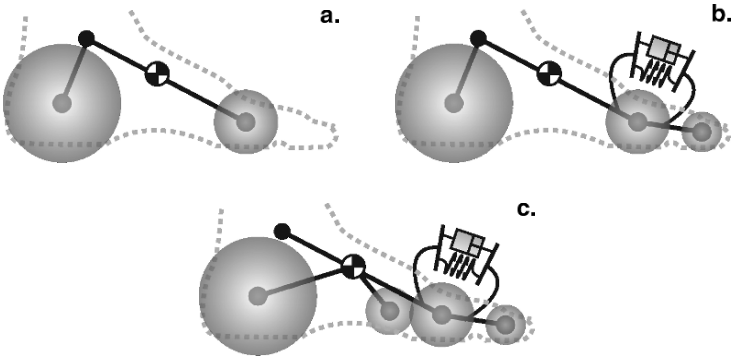

Fig. 5. Foot contact models consisting of two, three, and four spheres shown in a, b, and c. Models a and b have been tested; model c is hypothesized to be the least sensitive to changes in walking velocity

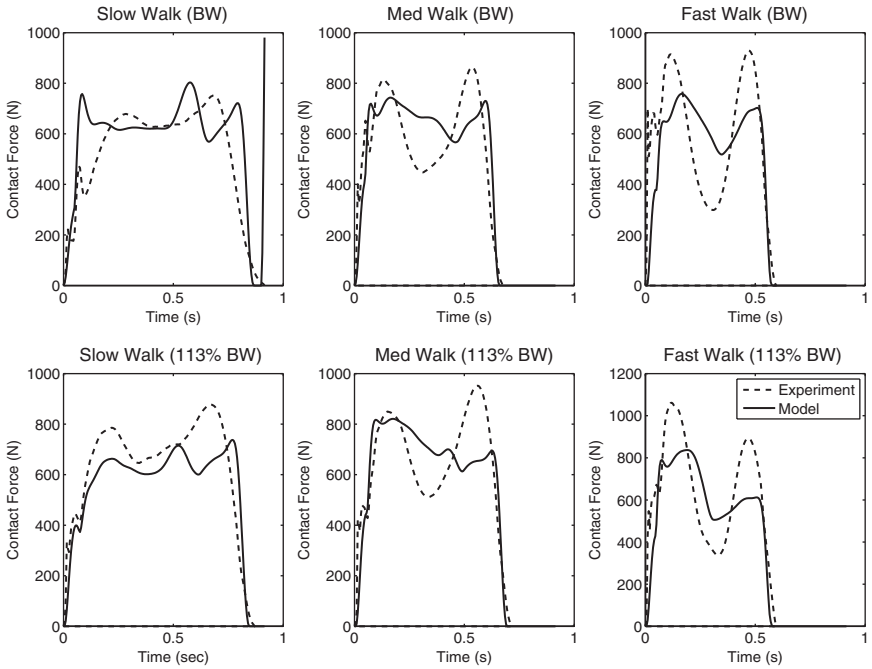

Fig. 6. The normal force developed between the two-sphere foot-contact model. 'BW' stands for 'bodyweight'

When the foot was tuned to fit the normal forces seen in each trial individually, a better result was obtained, however the geometry of the foot was different at every trial: the metatarsal contact was placed closer to the heel for the slow trials. One explanation for this behaviour lies in the role of toes: during slow walking the toes contribute very little to the normal force profile, shifting the average center of pressure of the forefoot towards the ankle. During fast walking the toes contribute more heavily to the normal force profile, shifting the average center of pressure of the forefoot towards the toes.

The friction forces predicted by the model were far below what was recorded during the experiment. Assuming that a Coulomb friction model was inadequate, a more advanced friction model was sought out. Bristle friction models [15] have been used as a substitute for Coulomb friction models in robotics simulations because both true stiction and conservative material shear can be simulated – which is in contrast to a Coulomb friction model that cannot model true stiction, nor conservative material shear. A bristle friction model mimics the forces developed between contacting bodies using the tangential displacement (z) and shear rate ($\dot{z}$) of viscoelastic bristles to generate friction forces as shown in Fig. 7 and in Eq. 5:

$$f_{br} = k_{br} z + a_{br} \psi(\dot{z}). \tag{5}$$

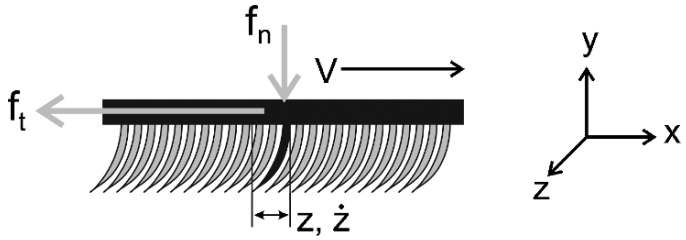

Fig. 7. A bristle friction model relies on the state of imaginary bristles on the surface of the contacting bodies to develop friction forces

The function $\psi(\dot{z})$ modulates the friction model from a bristle friction model for slip rates below the Stribeck velocity to a Coulomb friction model for slip rates above the Stribeck velocity. The 3D bristle friction model presented in [15] was employed, but without the dwell-time dependency.

The model produced encouraging normal contact force profiles in Fig. 6. Its performance indicated that toes may indeed play an important role in foot contact, and that a Coulomb friction model appears to be inadequate for modelling the tangential forces developed between the foot and the ground. In addition, the optimization routine should be constrained to find solutions that limit the compression of the foot pads to realistic levels.

5.6 Three-Sphere Two Segment Foot Contact Model

The foot contact model shown in Fig. 5b incorporated a toe segment (adding one dof to the model) to improve the normal ground reaction force profile, a bristle friction model to improve the friction force profile and parameter tuning routine was restricted to find solutions that had plausible compressions at the heel [10] and metatarsal [6] foot pads. Although the compressions seen at the heel and metatarsals contacts were kept to plausible levels, the normal ground reaction force profiles had a noticeably degraded performance relative to the previous model as shown in Fig. 8. The fast walking trials profiles resemble experimentally gathered normal ground reaction forces however, the model performs very poorly for the remainder of the trials – far worse than the previous model.

Some insight into why the previous two models produce the best results for the fast walking trials and poor results for the slow walking trials can be obtained by examining center-of-pressure (COP) of the subject's foot in the direction of travel shown in Fig. 9. The location of the COP has been plotted in Fig. 9 along with dividing lines marking the transitions from the heel to the mid-foot, the mid-foot to the 1st metatarsal pads and from the 1st metatarsal pad to the toes. Figure 9 clearly shows that the COP spends a significant amount of time in the mid-foot region for the slow trials, which progressively lessens as the walking speed increases. Figure 9 suggests that the models perform poorly for the slow trials because the mid-foot contributes

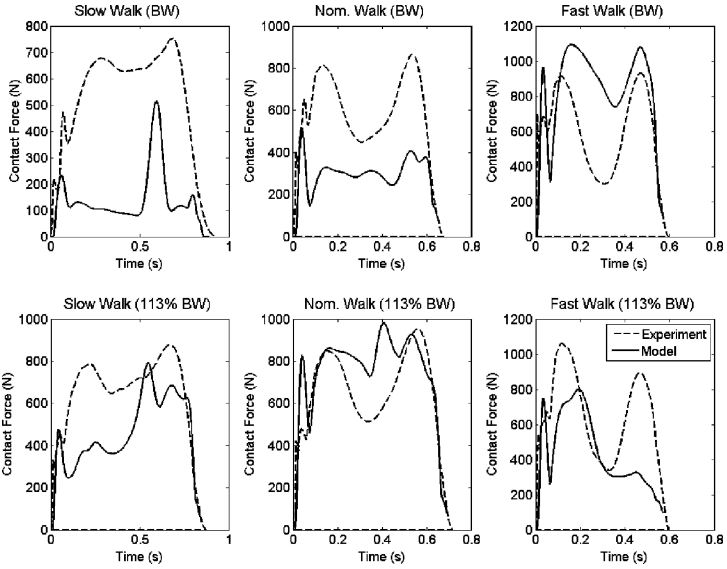

Fig. 8. The normal force developed between the three-segment foot-contact model with a toe contact

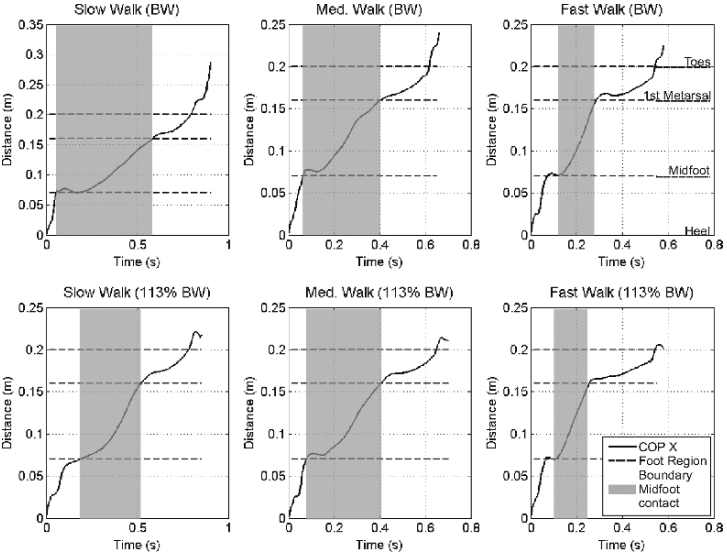

Fig. 9. The center of pressure in the direction of travel was segmented for each trial to show where the COP is relative to the foot. As the trials progress from slower to faster gaits, the COP is spending less and less time in the mid-foot region. This may explain why the contact models pictured in Fig. 5a, b. perform poorly at slow walking speeds: the tissue between the metatarsal and heel contacts is not being modelled

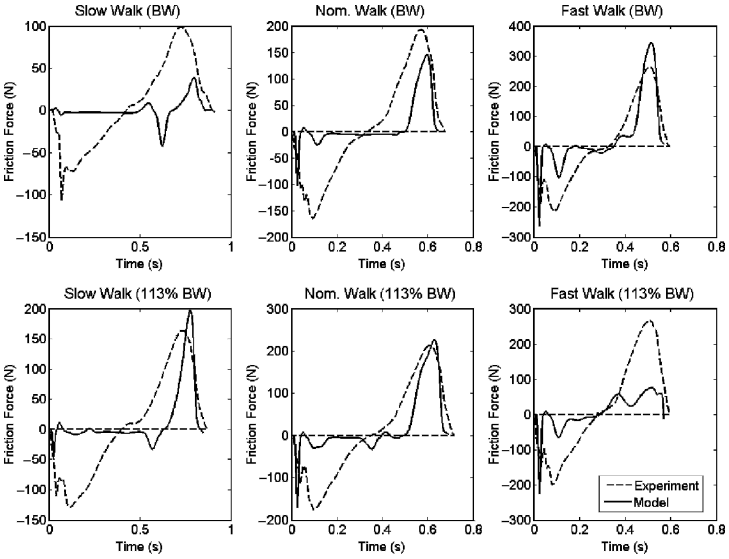

Fig. 10. Experimental and simulated friction force profiles, making use of a bristle friction model [15]

significantly to the normal contact force profile, yet this area of the foot is not being modelled. The previous two segment model performed better than the current three segment model because the compression levels of the foot pads was not restricted: the additional compression seen at the metatarsal contact allowed the model to artificially include the contribution of the mid-foot. The results of this model appear to indicate that it is necessary to model mid-foot contact. Accordingly a candidate foot contact model is shown in Fig. 5c that includes a mid-foot contact. This candidate foot contact model has yet to be implemented and tested.

The friction force profile shown in Fig. 10 was much improved over the Coulomb model, though failed to match all data sets shortly after foot contact and only roughly approximated the tangential forces towards the end of the foot contact. The poor representation of the friction force profiles may not be due to the model. The experimentally measured shear movements might also be too small to measure accurately: skin stretch and Optotrak IRED position error might be drowning the signal.

6 Conclusions

Multi-step, forward-dynamic human gait simulations do not yet have the fidelity to create precise predictions of how humans would walk in new situations. Peasgood et al.'s [23] system was a first attempt at developing a predictive human gait simulation. Although Peasgood et al.'s system was the first to

show that prosthetic gait has a greater metabolic cost than healthy gait *in silico* using a forward dynamic simulation, the predicted kinetics of Peasgood et al.'s healthy model were significantly different from published joint kinetics of human gait found using inverse dynamics analysis [26]. A high-fidelity kinetic response is required for high-fidelity gait predictions since metabolic cost is a function of muscle stress and thus joint torque: if the kinetic response of the model is poor, the model will not be able to converge to a human-like gait.

The joint torque profiles of the simulated gait are highly influenced by the ground reaction forces applied at the foot. Foot contact models were created using spherical elements and contact forces were calculated using Gonthier et al.'s volumetric contact model. The models were validated by driving the ankle joint through experimentally recorded ankle trajectories and examining the quality of match between the ground reaction forces developed at the simulated foot, and the human foot. Current modelling efforts indicate that it is important to represent the heel, mid-foot, and metatarsal foot pads in the contact model. It is important to note that it may not be possible to develop a 2D foot contact model that perfectly replicates the forces created between a 3D foot and the ground: foot roll in the frontal plane [5] is ignored in 2D. Additionally, a bristle friction model was found to predict foot friction forces better than a Coulomb friction model. The results of the bristle friction model were not ideal: it remains unclear if the friction model is inadequate or if noise in the experimentally collected foot kinematics is making this validation approach difficult.

The sensitivity of Peasgood et al.'s balance controller to initial conditions and joint trajectories prevented the gait space from being searched widely. Nearly six out of seven simulations resulted in a fall. High-fidelity predictive human gait simulations would benefit greatly from an advanced balance controller that is not sensitive to initial conditions, and is able to initiate, maintain, and terminate gait as adeptly as a human.

There is a lot of fundamental research that needs to be conducted before high-fidelity predictive human gait simulations can be developed. The predicted kinetics of a healthy human gait should follow those found using inverse dynamics [26]. Since the kinetics of the leg joints are highly influenced by the ground reaction forces at the foot, a high-fidelity foot contact model is required. Additionally, the model needs an advanced balance controller in order to search the gait space to find a metabolically minimal, or 'human-like' gait.

Acknowledgements

This research was supported by the Natural Sciences and Engineering Research Council of Canada. The authors would like to thank Mike Peasgood for his assistance with the MSC.Adams model and Mike MacLellan for his assistance with the experiments described in this paper.

References

1. Ackermann M, Schiehlen W (2006) Dynamic analysis of human gait disorder and metabolic cost estimation. Arch Appl Mech 75:569–594
2. Aerts P, Kerr RF, De Clecq D, Illsley DW, McNeil AR (1995) The mechanical properties of the human heel pad: a paradox resolved. J Biomech 28:1299–1308
3. Anderson F, Pandy M (1999) Static and dynamic optimization solutions for gait are practically equivalent. J Biomech 34:153–161
4. Anderson F, Pandy M (2001) Dynamic optimization of human walking. J Biomech Eng 123:381–390
5. Carson MC, Harrington ME, Thompson N, O'Connor JJ, Theologis TN (2001) Kinematic analysis of a multi-segment foot model for research and clinical applications: a repeatability analysis. J Biomech 34:1299–1307
6. Cavagna GA, Heglund NC, Taylor CR (1977) Mechanical work in terrestrial locomotion: two basic mechanisms for minimizing energy expenditure. Amer J Reg Integ Comp Phys 233(5):243–261
7. Cavanagh P (1999) Plantar soft tissue thickness during ground contact in walking. J Biomech 32:623–628
8. Crook AW (1952) A study of some impacts between metal bodies by a piezoelectric method. Proc Roy Soc Lond, Ser A 212:377–390
9. DynaFlexPro `http://www.maplesoft.com/dynaflexpro`. Accessed May 2, 2008
10. Gefen A, Megido-Ravid M, Itzchak Y (2001) In vivo biomechanical behavior of the human heel pad during the stance phase of gait. J Biomech 34:1661–1665
11. Gerritsen KGM, Bogert AV, Nigg BM (1995) Direct dynamics simulation of the impact phase in heel-toe running. J Biomech 28:661–668
12. Gilchrist L, Winter D (1996) A two-part viscoelastic foot model for use in gait simulations. J Biomech 29(6):795–798
13. Gilchrist L, Winter D (1997) A multisegment computer simulation of normal human gait. IEEE Trans Rehab Eng 5(4):290–299
14. Goldsmith W (1960) Impact: the theory and physical behavior of contacting solids. Edward Arnold, London
15. Gonthier Y, McPhee J, Piedboeuf J, Lange C (2004) A regularized contact model with asymmetric damping and dwell-time dependent friction. Mult Syst Dyn 11:209–233
16. Gonthier Y, McPhee J, Lange C, Piedboeuf JC (2007) On the implementation of coulomb friction in a volumetric-based model for contact dynamics. In: Proceedings of ASME IDETC, Las Vegas, NY, USA
17. Guler H, Berme N, Simon S (1998) A viscoelastic sphere model for the representation of plantar soft tissue during simulations. J Biomech 31:847–853
18. Hunt K, Crossley F (1975) Coefficient of restitution interpreted as damping in vibroimpact. Trans ASME J App Mech 42(E):440–445
19. Kinoshita H, Francis PR, Murase T, Kawai S, Ogawa T (1996) The mechanical properties of the heel pad in elderly adults. Eur J Appl Phys 73:404–409
20. Lewis R, Torczon V (1999) Pattern search algorithms for bound constrained minimization. SIAM J Optim 9(4):264–269
21. MSC.Adams `http://www.mscsoftware.com/products/adams.cfm`. Accessed May 2, 2008
22. MSC Software 2005r2 Contact. In: Adams/Solver Fortran help
23. Peasgood M, Kubica E, McPhee J (2007) Stabilization and energy optimization of a dynamic walking gait simulation. ASME J Comp Nonl Dyn 2:65–72

24. Taga G (1995) A model of the neuro-musculo-skeletal system for human locomotion. Biol Cybern 73:97–111
25. Valiant G (1984) A determination of the mechancial characteristics of the human heel pad in vivo. Ph.D. thesis, The Pennsylvania State University, State College, PA
26. Winter D (2005) Biomechanics and motor control of human movement. Wiley, Hoboken, NJ, 3rd edition
27. Wojtyra M (2003) Multibody simulation model of human walking. Mech Based Design Struct Mach 31(3):357–377
28. Zarrugh MY, Todd FN, Ralston HJ (1974) Optimization of energy expenditure during level walking. Eur J App Phys 33:293–306